Journal of The Electrochemical Society, **150** (2) A219-A228 (2003)
0013-4651/2003/150(2)/A219/10/$7.00 © The Electrochemical Society, Inc.

Nonflammable Methyl Nonafluorobutyl Ether for Electrolyte Used in Lithium Secondary Batteries

Juichi Arai*,z

Hitachi, Limited, Hitachi Research Laboratory, Ibaraki-ken 319-1292, Japan

Use of nonflammable methyl nonafluorobuyl ether (MFE) has been studied to develop an inherently safe electrolyte for lithium secondary batteries. A no flash point (NFP) solution was prepared by mixing a proper amount of MFE with a common electrolyte solvent such as dimethyl carbonate or ethyl methyl carbonate (EMC) and the NFP electrolyte was obtained by dissolving organic lithium salts (*e.g.*, $Li[SO_2C_2F_5]_2$; LiBETI) in the NFP solution. Cell capacities with NFP electrolyte of 1 mol dm^{-3} (M) LiBETI-MFE/EMC (80:20 vol %) were limited by the charge-discharge process on the graphite anode. Electrolyte components were investigated in terms of modifying the solid electrolyte interface film to improve the charge-discharge performance and cycle life of NFP electrolyte. Adding cyclic carbonate (*e.g.*, ethylene carbonate, EC) and $LiPF_6$ to the electrolyte reduced the interfacial resistance in a graphite/Li cell. A 18650 cylindrical cell with EC and $LiPF_6$ added to 1 M LiBETI-MFE/EMC (80:20) electrolyte discharged more than 90% of its capacity at a 1 C current rate (*vs.* the capacity at the 0.1 C) and kept more than 80% of its initial capacity after 560 cycles at the 1 C current rate and room temperature. Effects of these additives on charge-discharge capacities in a graphite/Li cell were also investigated in terms of electrochemical spectroscopy, X-ray photoelectron spectroscopy, solid-state ^{7}Li nuclear magnetic resonance, and attenuated total reflection infrared spectroscopy.
 [DOI: 10.1149/1.1538224]

Manuscript submitted February 19, 2002; revised manuscript received September 6, 2002. Available electronically January 9, 2003.

Lithium secondary batteries are indispensable power sources for portable electronic devices and they have also been developed for powering electric vehicles (EVs).[1,2] Lithium secondary batteries require organic solvents having high oxidation durability for the electrolyte because they are operated above the oxidation voltage of water (1.27 V). Organic electrolyte solvents are a safety concern in lithium secondary batteries due to their high flammability. For instance, ethyl methyl carbonate (EMC), a common electrolyte solvent used for these batteries,[3-5] has a flash point (FP) of 23°C. Though commercial lithium batteries are firmly based on safety devices such as a positive temperature coefficient (PTC, or thermal switch) device and a current intermitted device (CID), a low FP itself is a critical issue for safety when the batteries are crushed. Thus, an inherently safe battery is desired using no flash point (NFP) or nonflammable electrolytes.

Challenges to the development of nonflammable electrolytes have been made by use of fire-retardant additives[6-8] and nonflammable solvents.[9-12] Depression of the heat generation at elevated temperature by adding hexamethoxycyclotriphosphazene $[PN(OCH_3)_2]_3$ to 1 mol dm^{-3} (M) $LiPF_6$-EC/DMC electrolyte was measured with an ARC (accelerating rate calorimeter).[6] Trimethylphosphate $(CH_3O)_3P{=}O$ (TMP) was investigated both as a fire-retardant additive[7,8] and a nonflammable solvent.[9-11] Adding TMP to conventional electrolytes depressed the burning rates of the electrolyte according to UL94-based examination.[7] Using TMP as a cosolvent for the electrolyte (*e.g.*, a mixture of EC/DEC/TMP = 4/4/2 in volume) reduced the heat generation of the graphite/$LiCoO_2$ cell,[9] but CH_4 gas generation during the charge on the graphite anode due to the decomposition of TMP was a critical issue for its application.[10,11] Though these approaches effectively improve safety of lithium secondary batteries, these electrolytes still have FPs and thus a possibility to burst into flame.

Our idea for an inherently safe battery is use of nonflammable solvent as the main component of the electrolyte to reduce the flammability and eliminate FP.[12] We have investigated trifluoropropylene carbonate (TFPC) and chloroethylene carbonate (ClEC) mixed solvent electrolytes without any low FP cosolvents.[13] We eliminated the electrolyte FP by using a nonflammable solvent of methyl nonafluorobuyl ether CH_3-O-C_4F_{19} (MFE) as the main component of the electrolyte solvent (>80 vol % for MFE/EMC mixture).[12] The 1 M LiBETI ($LiN[SO_2C_2F_5]_2$)-MFE/EMC (80:20 vol %) is representative of novel electrolytes having no FP, which we proposed. Using this electrolyte, we investigated charge-discharge performances and cycle life of a graphite/$LiCoO_2$ 18650 cylindrical cell. The cell discharged almost the same capacity (1400 mAh) as the cell using 1 M $LiPF_6$-EC/EMC (30:70 vol %) at a 0.1 C rate (140 mA), though it discharged less than 800 mAh at a 0.9 C rate. The better safety obtained using this electrolyte was demonstrated in a nailing test. The cell using this electrolyte did not show thermal runaway when a nail penetrated it even when the cell was overcharged. The discharge capacities faded significantly after around 50 cycles in a cycle life test with a 0.1 C rate.

This paper focuses on improvement of the cell performances using 1 M LiBETI-MFE/EMC (80:20 vol %), by modifying the electrolyte components to enhance the Li^+ transport rate at the solid electrolyte interface (SEI) in terms of adding cyclic carbonates and $LiPF_6$. We present charge-discharge performances of 1 M LiBETI-MFE/EMC (80:20 vol %) and modified electrolytes in graphite/Li, $LiCoO_2$/Li, and graphite/$LiCoO_2$ cells. Electrochemical impedance spectroscopy (EIS), solid state ^{7}Li nuclear magnetic resonance (NMR), X-ray photoelectron spectroscopy (XPS), and attenuated total reflection infrared spectroscopy (ATR-IR) measurements were made to analyze the lithium intercalated states in the graphite anode and the SEI film on the electrode for the cells using LiBETI-MFE/EMC and its modified electrolytes. The cell performances including the rate capability and cycle life with the 18650 cylindrical cell are studied for MFE/EMC electrolyte with and without the additives.

Experimental

Chemical structures of electrolyte solvents are shown in Fig. 1. MFE is a semifluorinated ether and the main component of NFP electrolyte. Physical properties of MFE are summarized in Table I, with data of EMC for comparison. MFE features not only NFP but also has a wide temperature range for the liquid phase, and low viscosity and low surface tension. These are desirable properties for an electrolyte solvent, but MFE has a high density due to the fluorinated group. MFE mixes well with a solvent having a low dipole moment such as dimethyl carbonate (DMC), diethyl carbonate (DEC) or EMC (Fig. 1b). We obtained the NFP mixed solutions with these linear carbonates and MFE from certain mixing ratios as summarized in Table II.[12] In this study, we chose cyclic carbonates for electrolyte additives in order to improve the cell performances because cyclic carbonates are known as SEI film precursors,[14,15] though their miscibility in MFE is limited.[12]

* Electrochemical Society Active Member.
z E-mail: jarai@hrl.hitachi.co.jp

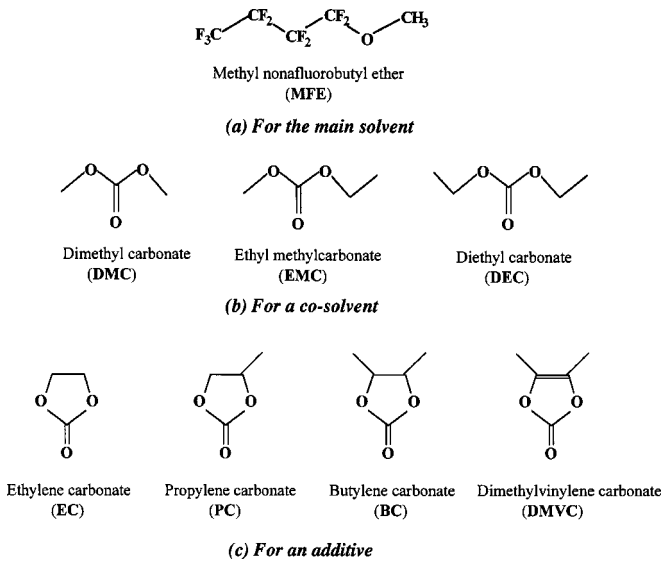

Figure 1. Chemical structures of electrolyte solvents: (a) the main solvent MFE, (b) cosolvents, and (c) additives.

Electrolyte preparations.—The electrolytes were prepared by mixing MFE (3 M Company) with EMC (Tomiyama) by volume percent, and dissolving LiBETI (lithium bis[pentafluoroethylsulfonyl] imide, 3 M Company) adjusting to 1 M concentration. The additives of ethylene carbonate (EC), propylene carbonate (PC), and butylene carbonate (BC) were purchased from Tomiyama. Dimethylvinylene carbonate (DMVC) was provided by Midori Kagaku. $LiPF_6$ (Hashimoto) was also used as an additive. The electrolyte preparation and storage were done in an Ar-filled glove box kept at less than −80°C of the dew point of water. The LiBETI was vacuum dried for more than 24 h at 120°C prior to use.

Cell fabrications and electrochemical measurements.—The anode was prepared by coating and drying the NMP (*N*-methyl pyrrolidone) paste composed of synthetic graphite (90 wt %) and poly vinylidene fluoride (PVDF) binder (10 wt %) on a copper foil. The cathode was formed on an aluminum foil by coating and drying the NMP paste which contained $LiCoO_2$ (85 wt %), graphite as electrical conducting supporter (8 wt %), and PVDF as binder (7 wt %). Graphite/Li, $LiCoO_2$/Li, and graphite/$LiCoO_2$ test cells were assembled with 1.76 cm^2 electrodes and 25 μm thick polyethylene (PE) separator. Graphite/$LiCoO_2$ 18650 cylindrical cells were fabricated by connecting the rolled the electrodes with the PE separator and putting them into a cell can. Then the electrolytes were injected separately after degassing the inside of the cell. Charge-discharge performances of the test cells were measured with a Hokuto Denko HJ-101 SM6 battery controller. EIS measurements of the test cells were carried out using a Solartron SI1286 poteniostat-galvanostat and SI1260 impedance/gain-phase analyzer controlled by a computer installed with a Pentium II processor and the measurement software ZPlot and Corrware. The EIS measurements were made from 1 MHz to 5 mHz. The charge-discharge performance values of the graphite/$LiCoO_2$ 18650 cylindrical cells were measured with a Toyo System 3000U battery controller.

Table I. Physical properties of MFE and EMC.

Solvent	Methyl nonafluorobutyl ether (MFE)	Ethyl methyl carbonate (EMC)
Molecular weight	250	104
Melting point (°C)	−135	−55
Boiling point (°C)	60	107
Flash point (°C)	NFP	23
Viscosity (10^7 m^2 s^{-1})	3.8	7.0
Surface tension (10^3 N m^{-1})	14	27
Density (kg dm^{-3})	1.52	1.01

Table II. FPs of MFE and cosolvent mixtures.

Volume fraction of MFE (vol %)	FP (°C)		
	DMC	EMC	DEC
0	17	23	33
70	41	58	NFP
80	NFP	NFP	NFP
90	NFP	NFP	NFP

Spectroscopic measurements.—^{7}Li-NMR spectra of graphite intercalated samples were obtained with a JEOL JNM-400GX spectrometer with magic angle spinning (MAS), and single pulse mode. An aqueous solution of LiCl was used for an external standard. The spinning speed of 5-6 kHz was achieved for all samples. XPS analysis of the electrode surface after a charge-discharge run for the test cells was carried out with the VG Scientific ESCALAB 220iXL spectrometer under ultrahigh vacuum (below 3×10^{-7} Pa). An Al Kα X-ray source was used (15 kV, 15 mA). The samples for XPS were dried under vacuum at 1×10^{-3} Pa for more than 12 h prior to the measurement to remove residual solvent. The binding energy of the neutral C 1s peak at 284.6 eV was used as an internal standard to calibrate the binding energy scale. ATR-IR spectra of the electrode surface were measured by a Bio Rad Digilab FTS-55A spectrometer with a single-reflection Ge prism attachment under an Ar atmosphere. The incident angle of the IR beam was 45°. The resolution was set at 4 cm^{-1} and the integration of the scan was 512.

Results and Discussion

Charge-discharge performances and EIS analysis of MFE/EMC electrolyte.—Cell performances using 1 M LiBETI-MFE/EMC (80:20 vol %) has been studied as a representative of the nonflammable electrolytes.[12a] 1 M $LiPF_6$-EC/EMC (30:70 vol %) was selected as a reference electrolyte to compare cell performances. Charge-discharge performances of 1 M LiBETI-MFE/EMC (80:20 vol %) in $LiCoO_2$/Li and graphite/Li test cells were evaluated to find what was limiting the cell capacities. Figure 2 shows the charge-discharge voltage curves of 1 M LiBETI-MFE/EMC (80:20 vol %) and 1 M $LiPF_6$-EC/EMC (30:70 vol %) in the $LiCoO_2$/Li cells for the first run as a function of cell capacity. The cells were charged at a constant current of 0.28 mA cm^{-2} from the open circuit voltage (OCV) to 4.2 V and discharged at the same current from the OCV (achieved after 30 min rest from the end of the charge) to 2.7 V. 1 M $LiPF_6$-EC/EMC had 134 mAh g^{-1} charge and 127 mAh g^{-1} discharge capacities which resulted in 95% charge/discharge efficiency. 1 M LiBETI-MFE/EMC showed 137 mAh g^{-1} charge and 134 mAh g^{-1} discharge capacities with 97% charge/discharge efficiency. LiBETI-MFE/EMC electrolyte had the same charge-discharge performance as 1 M $LiPF_6$-EC/EMC in the $LiCoO_2$/Li cell. Thus, the cell capacities in MFE/EMC electrolytes may not be limited by the cathode reactions.

Figure 3 shows the charge-discharge voltage curves of 1 M LiBETI-MFE/EMC and 1 M $LiPF_6$-EC/EMC in the graphite/Li cells for the first run as a function of cell capacity. The cells were charged from the OCV to 5 mV and discharged from the OCV (achieved after 30 min rest from the end of the charge) to 1 V at a constant current of 0.28 mA cm^{-2}. 1 M $LiPF_6$-EC/EMC had more than 300 mAh g^{-1} charge and 280 mAh g^{-1} discharge capacities which led to 92% charge/discharge efficiency. By contrast, 1 M LiBETI-MFE/EMC had only 99 mAh g^{-1} charge and 74 mAh g^{-1} discharge capacities which resulted in 75% charge/discharge effi-

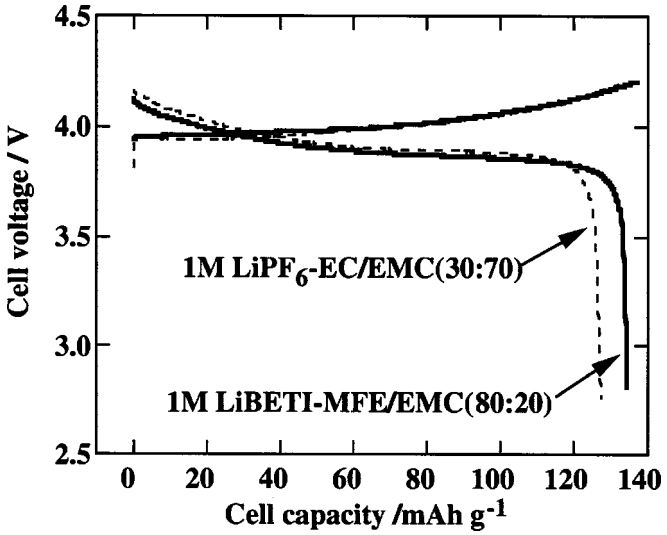

Figure 2. Voltage profiles in charge and discharge of the $LiCoO_2$/Li cells using 1 M LiBETI-MFE/EMC (80:20) and 1 M $LiPF_6$-EC/EMC (30:70) at 0.28 mA cm^{-2} current density.

ciency. The voltage curve indicated that there were large voltage drops in the graphite/Li cell using 1 M LiBETI-MFE/EMC during both the charge and discharge processes compared to the cell using 1 M $LiPF_6$-EC/EMC. Thus, the graphite anode had more influence on the capacity depression than the $LiCoO_2$ cathode when LiBETI-MFE/EMC was used.

The EIS measurements were made for the graphite/Li cells at the charged and discharged states to characterize the electrochemical properties for consideration of the difference between MFE/EMC and EC/EMC cells. Figure 4 shows the Cole-Cole plots for these cells. The R_s (an intercept value across the real part of impedance Z') in MFE/EMC (70-75 Ω cm^2) was larger than that in EC/EMC (*ca.* 5 Ω cm^2) due to the low ionic conductivity (*ca.* 0.5 mS cm^{-1}).[12] This affected the voltage profile and led to voltage drops in the charge-discharge processes as seen in Fig. 3. Assuming the interfacial resistance R_{ct} (the diameter of a slightly collapsed semicircle) was composed of one element, R_{ct} relates to the resistance in the ion transfer reaction.[16,17] The R_{ct} values measured at the

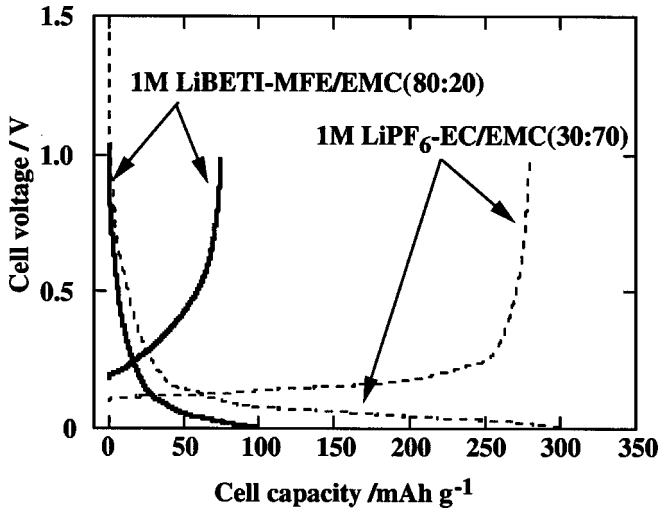

Figure 3. Voltage profiles in charge and discharge of the graphite/Li cells using 1 M LiBETI-MFE/EMC (80:20) and 1 M $LiPF_6$-EC/EMC (30:70) at 0.28 mA cm^{-2} current density.

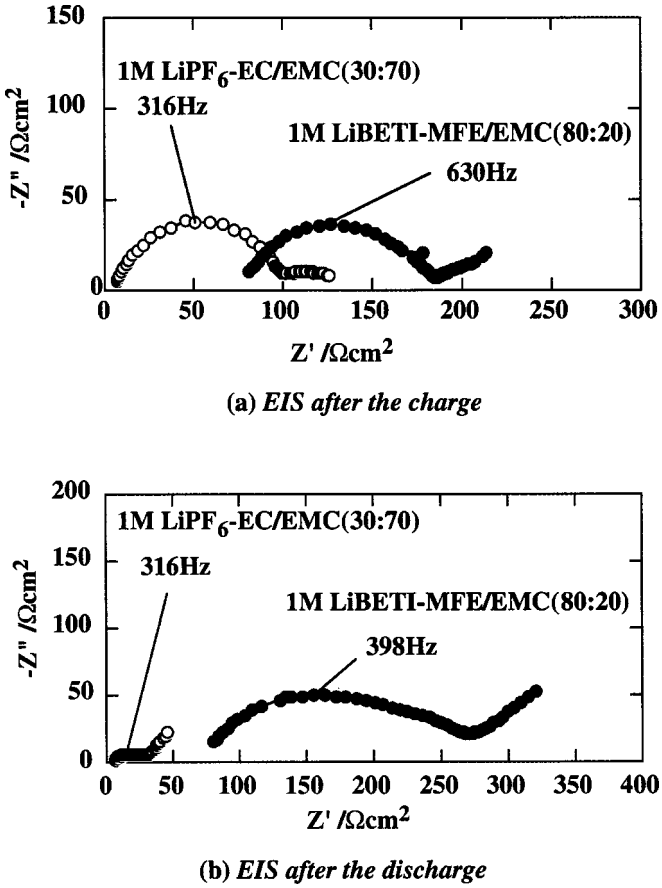

Figure 4. Cole-Cole plots of the graphite/Li cells using 1 M LiBETI-MFE/EMC (80:20) and 1 M $LiPF_6$-EC/EMC (30:70) measured after (a) charge and (b) discharge.

charged state (Fig. 4a) in MFE/EMC and EC/EMC were similar to each other. Thus, the ion transfer process may not regulate the cell capacities. The R_{ct} in MFE/EMC at the discharge state (240 Ω cm^2) was larger than that at the charge state (118 Ω cm^2), while the R_{ct} in EC/EMC at the charge state (100 Ω cm^2) became smaller at the discharge state (35 Ω cm^2). The characteristic frequency ω_o given at the peak of the semicircle is related to R_{ct} and C_d (double-layer capacitance, in general) as represented in Eq. 1

$$\omega_o = 1/(2\pi R_{ct} C_d) \quad [1]$$

The ω_o in MFE/EMC varied with charge (630 Hz) and discharge (398 Hz), while the ω_o in EC/EMC stayed constant (316 Hz). The R_{ct}, ω_o, and calculated C_d are listed in Table III. C_d is expressed in Eq. 2

$$C_d = \varepsilon_o \varepsilon_r / d \quad [2]$$

Here d is thickness of the layer and ε_o (8.85×10^{-14} F cm^{-1}) and ε_r represent permittivity in vacuum and relative dielectric constant of the material, respectively. The layer giving C_d may include the SEI film, solvent, and ion molecule absorbents in these systems. The composition which influences ε_r and thickness d of the layer varied with the charge and discharge processes in both cells. The thickness d in the MFE/EMC cell was more than twice thicker than that of the EC/EMC cell at the charge state, assuming both systems had the same ε_r value. Considering the ε_r values for fluorinated compounds are smaller than those for alkanes, the d in both cells might be close. The thickness d decreased in EC/EMC (to *ca.* 0.35 nm),[16] while the d increased in MFE/EMC (to *ca.* 1.28 nm) during the discharge

Table III. Estimated R_{ct}, ω_o, and C_d for EIS measured with 1 M LiBETI-MFE/EMC and 1 M $LiPF_6$-EC/EMC.

	After charge				After discharge			
Electrolyte	R_s (Ω cm^2)	R_{ct} (Ω cm^2)	ω_o (Hz)	C_d (μF cm^{-2})	R_s (Ω cm^2)	R_{ct} (Ω cm^2)	ω_o (Hz)	C_d (μF cm^{-2})
1 M LiBETI-MFE/EMC	5	118	630	2.14	5	240	398	1.67
1 M $LiPF_6$-EC/EMC	75	100	316	5.03	70	35	316	14.4

process if ε_r did not change. We thought that the modification of the SEI film (ε_r and d) was needed to decrease the resistance at low frequency, which would influence the charge-discharge processes and improve the cell capacities.

Charge-discharge performances and EIS analysis of MFE/EMC with additives.—We had to improve both R_s (related to ionic conductivity) and R_{ct} (related to the SEI film and structure of absorbents) for better charge-discharge performances of the MFE/EMC cell. But it was difficult to improve the ionic conductivity, because solvents having a higher dipole moment (and thus expected to realize higher solvation and higher dissociation than solvents having a low dipole moment) were not mixed at more than a few volume percents with MFE.[12] We focused on the progress of R_{ct} by the addition of high dipole moment (or high permittivity) compounds and $LiPF_6$, because the C_d may be reduced if the ε_r of the SEI becomes larger by including the products from the decomposition of these additives, according to Eq. 2.

The electrolytes of 1 M LiBETI-MFE/EMC (80:20 vol %) with 0.5 M EC, PC, BC, or DMVC were prepared. This concentration was almost the maximum value at which a uniform electrolyte solution could be sustained. Figure 5 shows the rate capability of graphite/$LiCoO_2$ test cells with these electrolytes, and 1 M LiBETI-MFE/EMC and 1 M $LiPF_6$-EC/EMC for comparison as a function of discharge current. The cells were charged to 4.1 V and discharged to 2.8 V at the current of 0.2, 0.4, 0.6, 0.8, 1, 2, and 3 C (1 C $\equiv$ 5 mA). The discharge capacities of the cell using LiBETI-MFE/EMC were significantly improved within a 1 C rate by the addition of EC, PC, and BC, although the improvement was insufficient when compared to $LiPF_6$-EC/EMC. At the 1 C rate, MFE/EMC + EC discharged 2.23 mAh, MFE/EMC + PC discharged 2.25 mAh, MFE/EMC + BC discharged 2.6 mAh, and MFE/EMC discharged 1.05 mAh. DMVC did not improve the cell capacities when operated at more than a 0.4 C rate. The double bond in DMVC seemed to affect the SEI film and cell capacities a lot because the only difference in chemical structure between BC and DMVC was the C-C bond order. It was unclear whether the reactivity of the double bond affected the cell capacities or the residual double bond in the reaction products did. The alkyl groups in EC (H), PC (CH_3), BC (two CH_3) did not seem to influence the cell capacities.

Then the effect of $LiPF_6$ addition was investigated. We added 0.1 M of $LiPF_6$ to 1 M LiBETI-MFE/EMC + EC (0.5 M) and 1 M LiBETI-MFE/EMC + PC (0.5 M). Figure 6 shows the rate capability of graphite/$LiCoO_2$ test cells using 1 M LiBETI-MFE/EMC + EC, 1 M LiBETI-MFE/EMC + EC + $LiPF_6$, 1 M LiBETI-MFE/EMC + PC, and 1 M LiBETI-MFE/EMC + PC + $LiPF_6$. The 1 M $LiPF_6$-EC/EMC was also used for comparison. $LiPF_6$ improved the rate capabilities of the cells with MFE/EMC + EC + $LiPF_6$ and MFE/EMC + PC + $LiPF_6$, and these cells were able to discharge at even a 3 C rate. In particular, MFE/EMC + EC + $LiPF_6$ discharged capacities comparable to 1 M $LiPF_6$-EC/EMC at all current rates. Thus, we determined that $LiPF_6$ was an additive which worked at higher current rates to enhance the discharge capacities.

Figure 7 shows the discharge capacities of graphite/$LiCoO_2$ test cells with 1 M LiBETI-MFE/EMC + EC + $LiPF_6$ at 1 and 2 C current rates as a function of $LiPF_6$ concentration. There was an optimum concentration of $LiPF_6$ to improve the rate capability. At 0.1 M $LiPF_6$, the rate capability of the cell using 1 M LiBETI-MFE/EMC + EC + $LiPF_6$ had its maximum discharge capacity. The reason for the rate capability drop at 0.2 M might be the instability of the electrolyte solution due to aggregation of EMC.[12] Adding more $LiPF_6$ induced phase separation in the MFE/EMC solution.

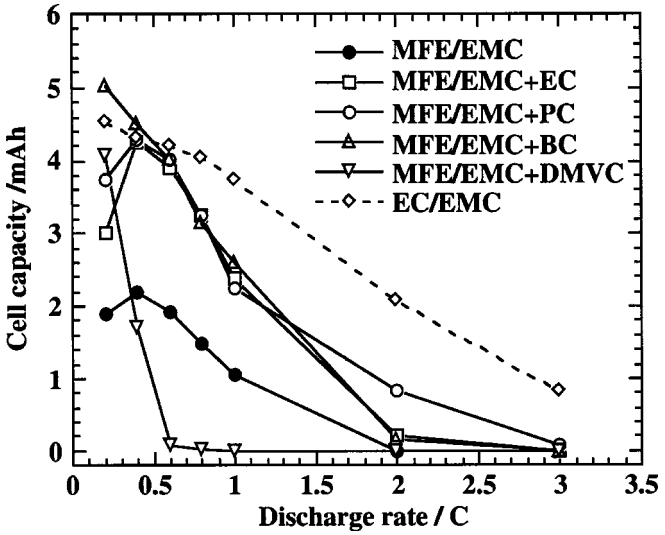

Figure 5. Rate capability of the graphite/$LiCoO_2$ cells using 1 M $LiPF_6$-EC/EMC, 1 M LiBETI-MFE/EMC, and 1 M LiBETI-MFE/EMC with EC, 1 M LiBETI-MFE/EMC with PC, LiBETI-MFE/EMC with BC, and LiBETI-MFE/EMC with DMVC.

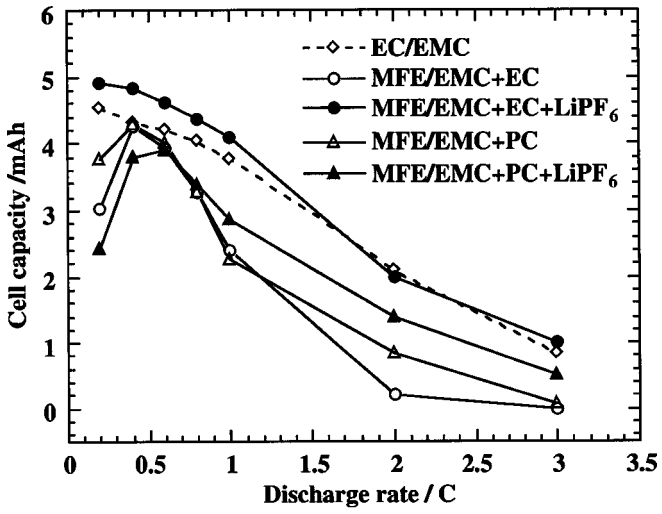

Figure 6. Rate capability of graphite/$LiCoO_2$ test cells using 1 M LiBETI-MFE/EMC + EC, 1 M LiBETI-MFE/EMC + EC + $LiPF_6$, 1 M LiBETI-MFE/EMC + PC, and 1 M LiBETI-MFE/EMC + PC + $LiPF_6$. 1 M $LiPF_6$-EC/EMC was also used for comparison.

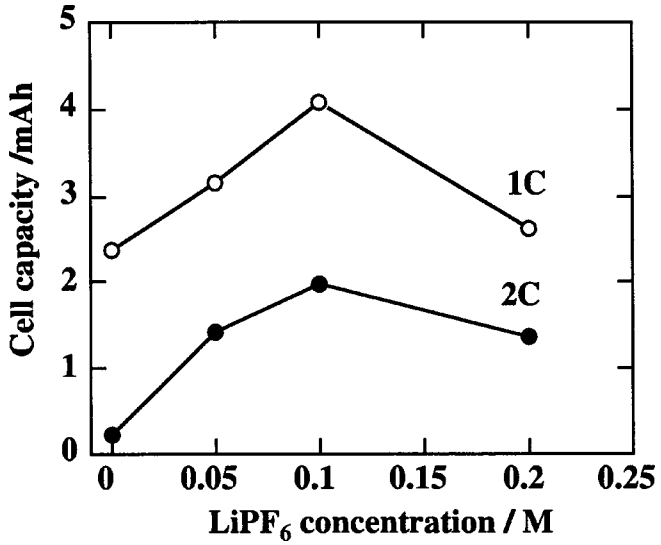

Figure 7. Cell discharge capacity as a function of $LiPF_6$ concentration in the graphite/$LiCoO_2$ cells with 1 M LiBETI-MFE/EMC + EC at 1 and 2 C discharge current rates.

The charge-discharge test of graphite/Li cells with 1 M LiBETI-MFE/EMC + EC and 1 M LiBETI-MFE/EMC + EC + $LiPF_6$ was carried out to verify the effect of additives. Figure 8 shows the voltage profiles of these cells and the cell with 1 M LiBETI-MFE/EMC for comparison as a function of cell capacities. The cell with 1 M LiBETI-MFE/EMC + EC charged 98 mAh g^{-1} and discharged 78 mAh g^{-1}, leading to an 80% charge-discharge efficiency. This charge capacity was almost the same as the cell with 1 M LiBETI-MFE/EMC (99 mAh g^{-1}), but the efficiency was improved 5% compared to the MFE/EMC system (efficiency 75%). The cell with 1 M LiBETI-MFE/EMC + EC + $LiPF_6$ charged 121 mAh g^{-1} and discharged 99 mAh g^{-1}, and had an 81% charge-discharge efficiency. The charge capacity was much improved compared to the other electrolyte systems, by about 23 mAh g^{-1}, compared to the other electrolyte systems, while keeping the charge-discharge efficiency at that of the MFE/EMC + EC system. Thus, EC may effect the charge-discharge efficiency and $LiPF_6$ may play an important role in the charge process.

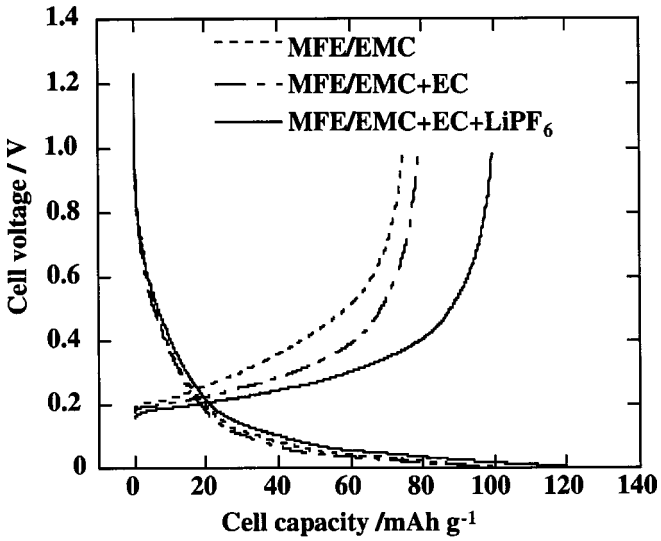

Figure 8. Voltage profiles in charge and discharge of the graphite/Li cells using 1 M LiBETI-MFE/EMC + EC, 1 M LiBETI-MFE/EMC+EC +$LiPF_6$, and 1 M $LiPF_6$-EC/EMC at 0.28 mA cm^{-2} current density.

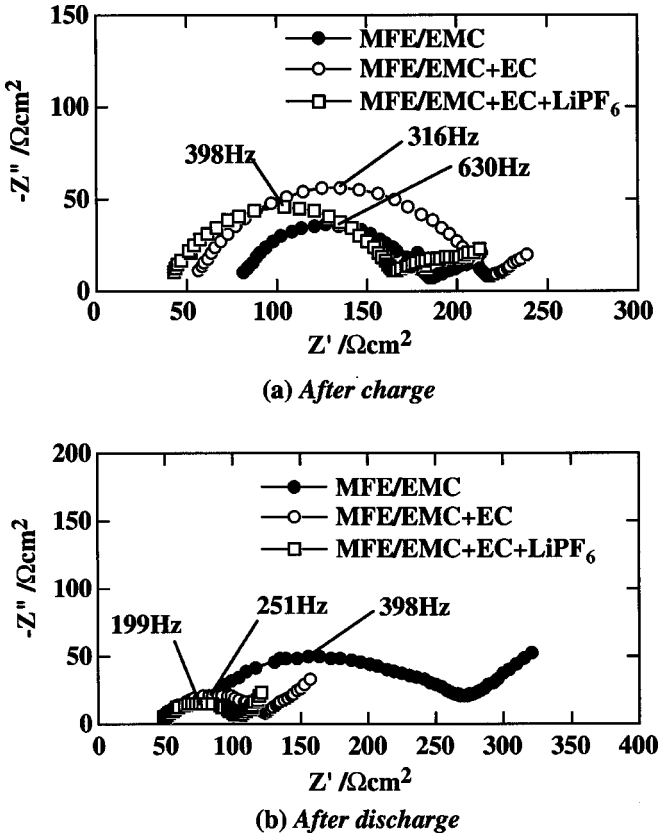

Figure 9. Cole-Cole plots of the graphite/Li cells using 1 M LiBETI-MFE/EMC + EC, 1 M LiBETI-MFE/EMC + EC + $LiPF_6$, and 1 M $LiPF_6$-EC/EMC measured after (a) charge and (b) discharge.

We measured the EIS of these cells after charge and discharge to characterize the electrochemical properties of SEI films. Figure 9 shows the Cole-Cole plots of EIS measured after (a) charge and (b) discharge for these cells. The estimations of R_s, R_{ct}, ω_o, and C_d are listed in Table IV. The R_s of MFE/EMC (75 Ω cm^2 for charge and 70 Ω cm^2 for discharge) were significantly reduced by adding EC (48 Ω cm^2 for charge and 44 Ω cm^2 for discharge). Adding $LiPF_6$ further reduced the R_s (36 Ω cm^2 for charge and 40 Ω cm^2 for discharge). These additives stabilized the R_{ct} during the charge-discharge processes. The R_{ct} in the MFE/EMC cell increased from 118 Ω cm^2 (charge) to 240 Ω cm^2 (discharge). The R_{ct} in MFE/EMC + EC cell decreased from 174 Ω cm^2 (charge) to 110 Ω cm^2 (discharge). The R_{ct} in the MFE/EMC + EC + $LiPF_6$ cell decreased from 136 Ω cm^2 (charge) to 94 Ω cm^2 (discharge). These changes in the cells using MFE/EMC with additives were the same as results obtained with the conventional electrolyte of 1 M $LiPF_6$-EC/EMC (Fig. 4). The C_d also increased by addition of EC and $LiPF_6$ (see Table III). This suggested that the thickness d of the SEI films was reduced or the ε_r of the SEI was changed, for example, by inclusion of the reaction products of these additives in the SEI. The SEI films with additives were strong enough to prevent further reaction (decomposition) in MFE/EMC system. Thus, the addition of EC and $LiPF_6$ affected both R_s and R_{ct}, leading to better electrochemical properties in the SEI films and larger charge-discharge capacities.

Spectroscopic analysis of graphite anodes with MFE/EMC electrolytes.—To characterize the charge (Li intercalation) state with

Table IV. Estimated R_{ct}, ω_o, and C_d for EIS measured with 1 M LiBETI-MFE/EMC + EC and 1 M LiBETI-MFE/EMC + EC + $LiPF_6$.

	After charge				After discharge			
Electrolyte	R_s (Ω cm^2)	R_{ct} (Ω cm^2)	ω_o (Hz)	C_d (μF cm^{-2})	R_s (Ω cm^2)	R_{ct} (Ω cm^2)	ω_o (Hz)	C_d (μF cm^{-2})
1 M LiBETI-MFE/EMC + EC	48	174	316	2.89	44	110	251	5.78
1 M LiBETI-MFE/EMC + EC + $LiPF_6$	36	136	398	2.94	40	94	199	8.51

MFE/EMC electrolytes, ^{7}Li MAS-NMR measurements of the charged graphite with MFE/EMC electrolytes and 1 M $LiPF_6$-EC/EMC were performed (Fig. 10). The peaks at around 45 ppm, seen in all spectra, were attributed to LiC_6 (the first stage).[18] Peaks which appeared from 14 to 18 ppm were attributed to LiC_{18} (the third or higher stage). The peaks at around −30, −4, 73, and 97 ppm were satellite bands of the main peak. The graphite anode charged with EC/EMC showed only the LiC_6 peak. The graphite anodes charged with MFE/EMC electrolytes possessed not only the peaks due to LiC_{18} but also LiC_6, though they had small charge capacities (*e.g.*, 99 mAh g^{-1} for 1 M MFE/EMC) compared to the other system (a 45 ppm peak was found in a carbon fiber anode charged with 1 M $LiClO_4$-EC/DEC (1/1 vol %) from the capacity of 230 mAh g^{-1}).[18] Comparing the peak ratio of LiC_6 to LiC_{18} among the spectra charged with MFE/EMC electrolytes, we saw LiC_6 clearly increased in the anode charged with 1 M MFE/EMC + EC and 1 M MFE/EMC + EC + $LiPF_6$. Thus, EC and $LiPF_6$ not only improved the charge capacity of MFE/EMC electrolyte, but also realized higher density stages of lithium intercalation.

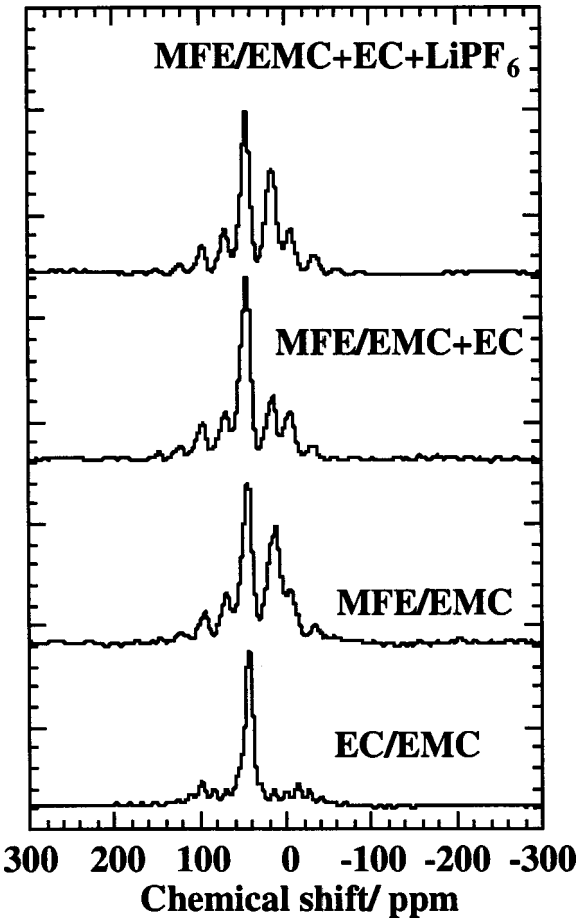

Figure 10. ^{7}Li MAS-NMR spectra of the graphite charged using 1 M LiBETI-MFE/EMC, 1 M LiBETI-MFE/EMC + EC, 1 M LiBETI-MFE/EMC + EC + $LiPF_6$, and 1 M $LiPF_6$-EC/EMC recorded with external standard of LiCl.

To characterize the SEI films, the ATR-IR and XPS of the graphite anodes charged with MFE/EMC electrolytes and EC/EMC were measured for samples after being charged and discharged under the same conditions described in the previous section. Figure 11 shows the ATR-IR spectra measured after (a) charge and (b) discharge. The characteristic peaks observed in the spectra measured for EC/EMC were the >C = O stretching at 1810 and 1780 cm^{-1}, the C-O stretching at around 1300 cm^{-1}, and the CH_x bending at around 1400 cm^{-1}.[14,19,20] These peaks indicated the existence of carbonate compounds (EC and EMC) or reaction products of carbonate compounds. The spectra for EC/EMC did not change much during the discharge, indicating that the SEI film formed with this electrolyte was stable.

The spectra of samples charged with MFE/EMC electrolytes differed from those for EC/EMC. Comparing the absorbance intensity of these spectra, we thought that the thickness of the SEI film formed on these anodes was on the order of EC/EMC < MFE/EMC + EC < MFE/EMC + EC + $LiPF_6$ < MFE/EMC. This order was in good agreement with the order of magnitude of R_{ct} measured after discharge in the EIS. Thus, the thickness d of the SEI film might vary with the electrolyte components. EC and $LiPF_6$ may inhibit growth of SEI film in the MFE/EMC system.

The IR spectra of SEI films formed in the cell with $LiN[SO_2CF_3]_2$-containing electrolytes were assigned as follows: a peak around 1330 cm^{-1}, stretching of SO_2(-N); a peak around 1245 cm^{-1}, asymmetric stretching of SO_2; a peak around 1140 cm^{-1}, symmetric stretching of SO_2; and a peak around 1060 cm^{-1}, stretching of S═O.[21] In the spectra observed for the anode charged with MFE/EMC electrolytes, we found peaks at around 1310, 1225, and 1178 cm^{-1}. These peaks must be ascribed to $N[SO_2CF_2CF_3]_2^-$ or its derivatives, considering the spectrum measured by the ATR method varied with the reflectance of the specimen. The peaks which appeared at around 1430 and 1650 cm^{-1} must be attributed to CH_x (wagging) and COO^- of salt formation such as ROCOO-Li. The main component of SEI formed on the anode with 1 M LiBETI-MFE/EMC electrolytes was found to be $N[SO_2CF_2CF_3]_2^-$ anion or its derivatives. Among the anodes charged with MFE/EMC electrolytes, the peak around 1650 cm^{-1} increased by adding EC and $LiPF_6$. Thus, these additives affected the SEI by forming compounds having a COO^- group. These species might have a small ε_r and an enhanced C_d to lead to the lower ω_o in the Cole-Cole plots for the cells charged and discharged with MFE/EMC + EC and MFE/EMC + EC + $LiPF_6$ compared to MFE/EMC.

Figure 12 shows the C 1s XPS spectra of anode after being (a) charged and (b) discharged with MFE/EMC and EC/EMC electrolytes. The spectrum for the EC/EMC system after charging had peaks at around 289.5, 286.5, and 284.5 eV attributed to CF_2 due to PVDF binder, CH_2 due to PVDF binder, and CH_x due to the reaction products of solvents, respectively. In this anode specimen, the main component of the SEI film was clearly found to be CH_x.[22] In the spectrum for this electrolyte system after discharge, the peak at 284.5 eV became smaller and a new peak which appeared at around 293.5 eV was attributed to CF_3. Additionally, the peaks due to

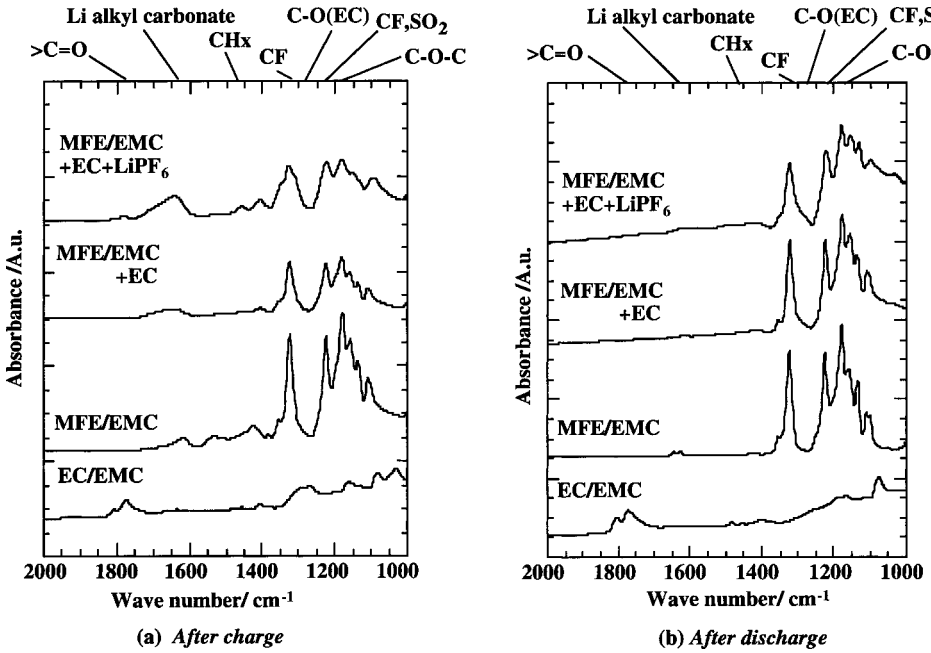

Figure 11. ATR-IR spectra of the graphite anodes measured after (a) charge and after (b) discharge using 1 M LiBETI-MFE/EMC, 1 M LiBETI-MFE/EMC +EC, 1 M LiBETI-MFE/EMC + EC +$LiPF_6$, and 1 M $LiPF_6$-EC/EMC.

PVDF became obvious. This suggested that the SEI film after the discharge became thinner than that after charge and some side reactions with PVDF took place during the discharge. This agreed with the change seen in the EIS measurements, where the resistance (R_{ct}) became smaller after the discharge than after the charge in EC/EMC electrolyte (see Fig. 4).

The spectra obtained with MFE/EMC electrolytes distinctively differed from the spectra given by EC/EMC electrolyte in Fig. 12a and b. The large peaks due to CF_3 (283.5 eV) and CF_2 (290.5 eV) suggested that the SEI film formed in MFE/EMC electrolytes included $N[SO_2CF_2CF_3]_2^-$ or its derivatives as found in the ATR-IR measurements, because the ratio of peaks at 289.5 and 286.5 eV was not equal (the ratio should be one, if it belonged to PVDF).[23] The large R_{ct} for MFE/EMC electrolytes in the EIS measurement might be related to these species. Among the spectra for MFE/EMC electrolyte after charge (Fig. 12a), the CH_2 (286.5 eV) and CH_x (284.5 eV) peaks increased by the addition of EC and $LiPF_6$. Thus, chemical species having these groups in the SEI films must have an effect to reduce the R_{ct} in the cells using MFE/EMC electrolytes. These peaks decreased in the spectra measured after discharge for MFE/EMC electrolytes, except for MFE/EMC electrolyte without the additives (Fig. 12 b). These chemical species of CH_2 and CH_x may act to reduce the R_{ct} after charge but to enlarge it after discharge. Thus, EC and $LiPF_6$ gave highly conductive SEI film components during the charge.

Figure 13 shows the P 2p XPS spectra for the anode during charge-discharge with (a) 1 M LiBETI-MFE/EMC + EC + $LiPF_6$ and (b) 1 M $LiPF_6$-EC/EMC. The peaks at *ca.* 134 and 137 eV were attributed to PO_3 and P-F, respectively.[22] PF_6^- derivatives were obviously included in the SEI film on the anode charged with 1 M LiBETI-MFE/EMC + EC + $LiPF_6$, as seen in Fig. 13a. Thus, we confirmed that SEI film was modified by the addition of $LiPF_6$. The peak intensity ratios between PO_3 and P-F in the specimen obtained with MFE/EMC (Fig. 13a) and that with EC/EMC (Fig. 13b) were different. The PO_3 peak was bigger than the P-F peak and even

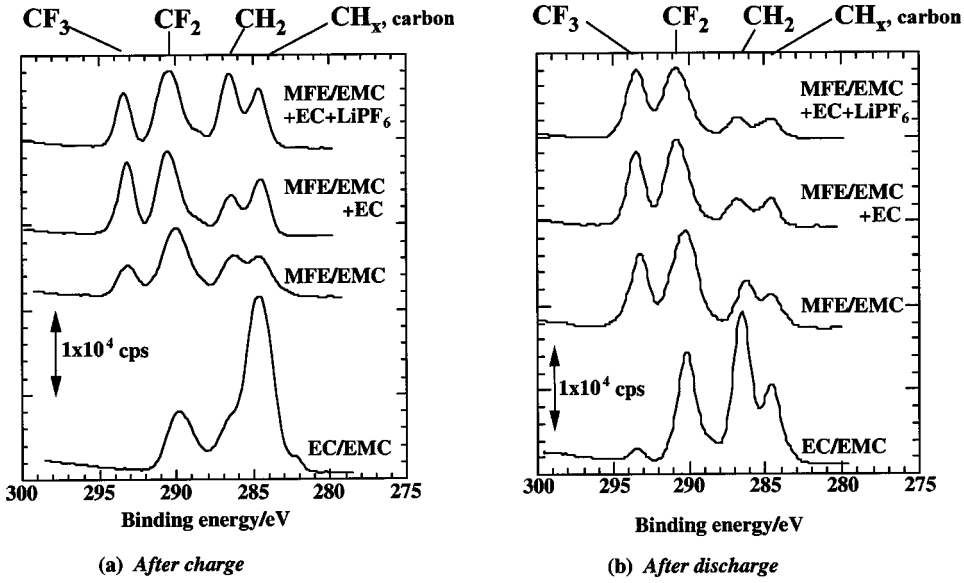

Figure 12. C 1s XPS spectra of the graphite anodes measured after (a) charge and after (b) discharge using 1 M LiBETI-MFE/EMC, 1 M LiBETI-MFE/EMC+EC, 1 M LiBETI-MFE/EMC + EC + $LiPF_6$, and 1 M $LiPF_6$-EC/EMC.

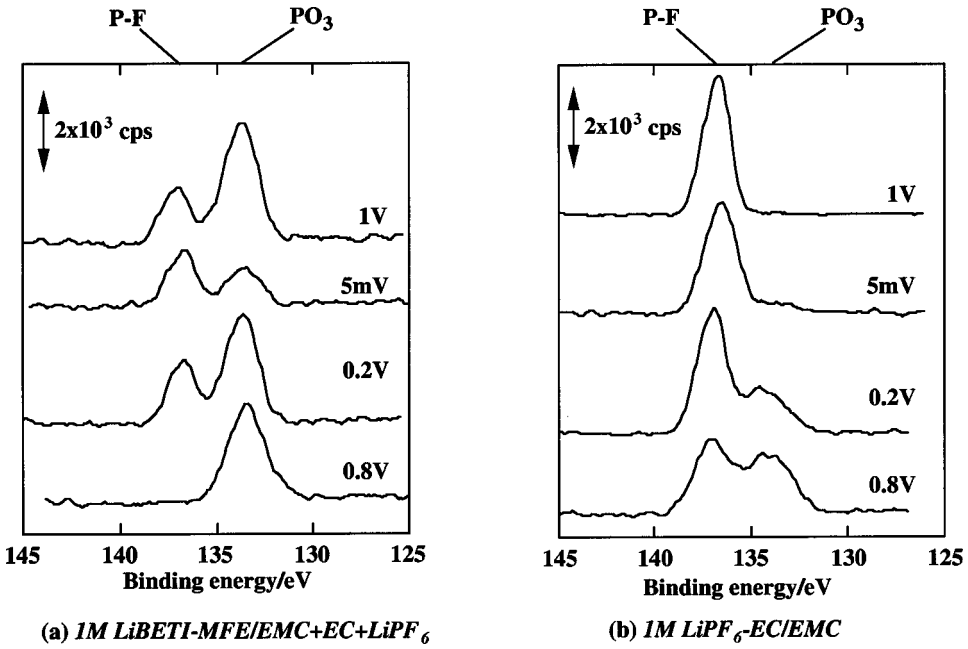

Figure 13. P 2p XPS spectra of the graphite anodes measured at various charge states and discharge states for (a) 1 M LiBETI-MFE/EMC + EC +$LiPF_6$ and (b) 1 M $LiPF_6$-EC/EMC.

remained at the end of the charge (5 mV) and after the discharge (1 V) in the anode operated with 1 M LiBETI-MFE/EMC + EC + $LiPF_6$. However, the PO_3 peak was only detected at the beginning of the charge (0.8-0.2 V), then disappeared at the end of the charge and after the discharge in the spectra for the anode run with 1 M $LiPF_6$-EC/EMC. We measured XPS of the surface of the SEI film at each charge-discharge state; thus, the facts meant that PO_3 species were present at the bottom of the film or just on the surface of the carbon. We thought that PF_6^- molecules were stacked by the other reaction products such as lithium alkyl carbonate in the SEI film at the beginning of the charge, and then they reacted with oxygen present on the surface of the carbon as drawn in Fig. 14. Though Ericksson *et al.*[22] suggested that PF_3O (around 135 eV) was derived from the reaction of PF_5 with residual H_2O in electrolytes for $LiMn_2O_4$ dissolution phenomena, we thought this was an electrochemical reaction because the PO_3 peak depended on the states of charge-discharge. After the PO_3 species grew to a layer of sufficient thickness, PF_6^- molecules did not react with oxygen anymore and P-F species increased in the film. The SEI film thickness d in EC/EMC seemed to be thicker than that in MFE/EMC + EC + $LiPF_6$ after the charge based on the peak intensity ratio. This suggested that the ε_r of SEI film formed with MFE/EMC + EC + $LiPF_6$ may be smaller than that of EC/EMC and the small ε_r resulted in the larger R_{ct} in the cell using MFE/EMC electrolytes, if the thickness d was the same in both SEI films.

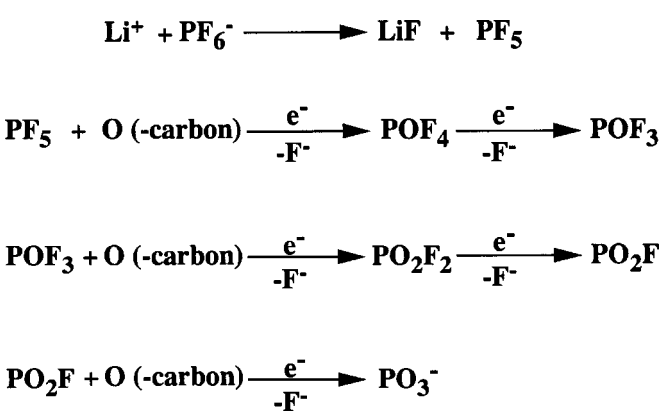

Figure 14. Suggested reaction scheme for the generation of PO_3^- from $LiPF_6$ by electrochemical reactions.

18650 cylindrical cell performances of MFE/EMC with additives.—We evaluated the cell performances using 1 M LiBETI-MFE/EMC + EC + $LiPF_6$ with the 18650 cylindrical cell. Figure 15 shows the rate capability of 18650 cells with 1 M LiBETI-MFE/EMC + EC + $LiPF_6$, 1 M LiBETI-MFE/EMC, and 1 M $LiPF_6$-EC/EMC. The cells were charged at a constant current and constant voltage of 4.1 V with cutoff current limit of 20 mA, and discharged at a constant current with a selected current rate. 1 C was defined as 1400 mA. Up to 1.5 C, the cell with 1 M MFE/EMC + EC + $LiPF_6$ kept more than 90% capacity (*vs.* the capacity at 0.2 C), while the cell with 1 M LiBETI-MFE/EMC lost the capacity from 0.4 C. The rate capability of the cell with MFE/EMC was significantly improved by adding EC and $LiPF_6$, though

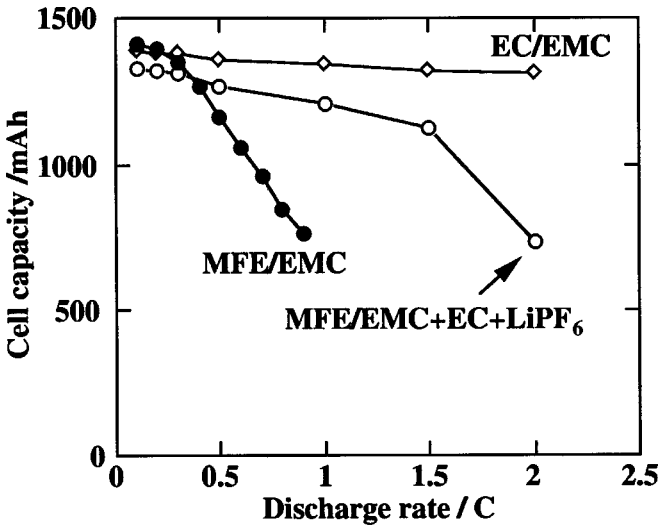

Figure 15. Rate capability of the graphite/$LiCoO_2$ 18650 cells using 1 M LiBETI-MFE/EMC, 1 M LiBETI-MFE/EMC + EC + $LiPF_6$, and 1 M $LiPF_6$-EC/EMC at 25°C.

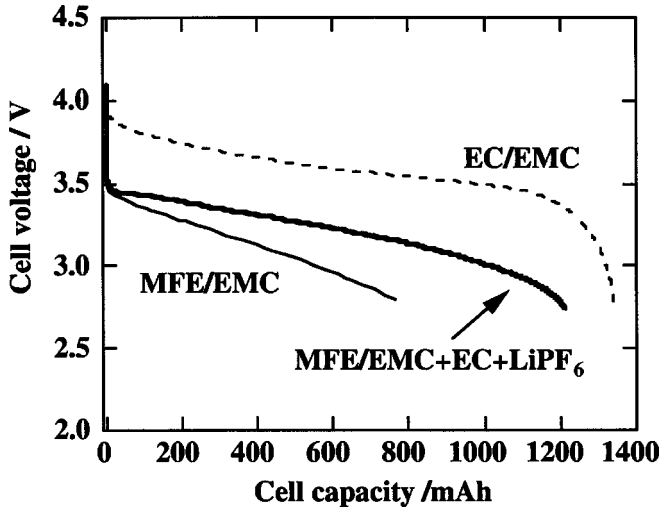

Figure 16. Voltage profiles in charge and discharge of the graphite/$LiCoO_2$ 18650 cells at 25°C using 1 M LiBETI-MFE/EMC, 1 M LiBETI-MFE/EMC + EC + $LiPF_6$, and 1 M $LiPF_6$-EC/EMC with 1 C (1400 mA) current rate.

the rate capability of the cell with MFE/EMC + EC + $LiPF_6$ was not enough if compared to that with 1 M $LiPF_6$–EC/EMC.

Figure 16 shows the discharge voltage profiles of the 18650 cells with 1 M LiBETI-MFE/EMC + EC + $LiPF_6$ and 1 M $LiPF_6$-EC/EMC at 1 C rate, and 1 M LiBETI-MFE/EMC at 0.9 C rate. The voltage profile of the cell with 1 M LiBETI-MFE/EMC + EC + $LiPF_6$ was close to that with 1 M $LiPF_6$-EC/EMC, except for the initial drop of voltage, while that with 1 M LiBETI-MFE/EMC had a steeper voltage drop. Thus, EC and $LiPF_6$ made R_{ct} smaller and sustained the discharge cell voltage. The initial voltage drop must be due to R_s and related to the conductivity of the electrolytes. We are still trying to resolve these points in terms of development of novel salts that should have a higher dissolution into MFE/EMC mixed solvent and higher dissociation in it than LiBETI.

Figure 17 shows results for the cycle life test at 25°C with (a) 0.1 and (b) 1 C rates. The cells were charged at a constant current and constant voltage (4.1 V) with cutoff current limit of 20 mA, and discharged at constant current to 2.8 V. The cycle life of the cell using 1 M LiBETI-MFE/EMC was significantly improved by adding EC and $LiPF_6$ at both low (0.1 C) and high (1 C) current rates. The cell using 1 M LiBETI-MFE/EMC + EC + $LiPF_6$ kept 93% of the initial capacity after 270 cycles, while the cell using 1 M LiBETI-MFE/EMC reached 80% of the initial capacity after 60 cycles in the 0.1 C cycle life test. The cell using 1 M LiBETI-MFE/EMC + EC + $LiPF_6$ kept more than 90% of the initial capacity even after 560 cycles. This cycle life was even better than the cell using 1 M $LiPF_6$-EC/EMC. LiBETI is known to react with aluminum cathode current collector and dissolve it above *ca.* 4.1 V,[24-26] but solvents having low dipole moment depress the reaction rate of this reaction.[25,26] Thus, MFE may have an effect on this point and prevent the dissolution reaction of aluminum by LiBETI, leading to good cyclability. PO_3 in the SEI film on the carbon anode may prevent the successive decomposition of 1 M LiBETI-MFE/EMC and $LiPF_6$ would inhibit the aluminum corrosion.

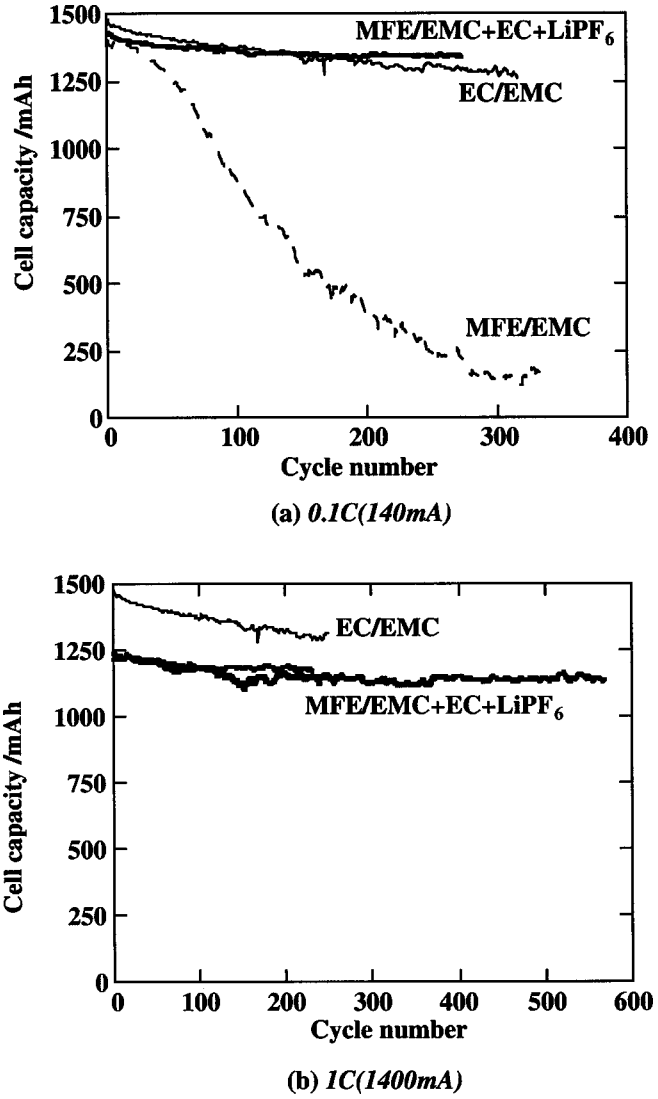

Figure 17. Cycle life of the graphite/$LiCoO_2$ 18650 cells at 25°C using 1 M LiBETI-MFE/EMC, 1 M LiBETI-MFE/EMC + EC + $LiPF_6$, and 1 M $LiPF_6$-EC/EMC with (a) 0.1 and (b) 1 C current rate.

Conclusions

To improve cell performances using NFP electrolytes containing MFE for better safety of lithium secondary batteries, we investigated the electrolyte component using several additives. The charge-discharge capabilities of the cell using 1 M LiBETI-MFE/EMC (80:20 vol %) were controlled by the charge-discharge reaction in the graphite anode. No such capacity limitation was found in the $LiCoO_2$/Li cell using the electrolyte when compared to 1 M $LiPF_6$-EC/EMC. Adding cyclic carbonates, EC, PC, and BC as an SEI film precursor, we saw the rate capability of the cell using the electrolyte was substantially improved. Addition of $LiPF_6$ together with cyclic carbonate improved the rate capability even further. The EIS measurements revealed that these additives reduced not only the R_{ct} but also R_s in the graphite/Li cell using 1 M LiBETI-MFE/EMC electrolytes. The ATR-IR spectra indicated that EC and $LiPF_6$ increased the amounts of lithium carbonates in the SEI film formed on the graphite anode charged with 1 M LiBETI-MFE/EMC + EC and 1 M LiBETI-MFE/EMC + EC + $LiPF_6$. The XPS measurements indicated that the LiBETI derivatives were the dominant components of the SEI film formed with 1 M LiBETI-MFE/EMC electrolytes, and $LiPF_6$ derivatives clearly existed in the film formed with 1 M LiBETI-MFE/EMC + EC + $LiPF_6$. The improvement of rate capability and cycle life was demonstrated with the graphite/$LiCoO_2$ 18650 cylindrical cell using 1 M LiBETI-MFE/EMC + EC + $LiPF_6$. The cell discharged more than 90% of the capacity (*vs.* the capacity obtained at 0.1 C) at 1.5 C, and kept more than 90% of the initial capacity after 560 cycles in the 1 C cycle life test. We

believe that 1 M LiBETI-MFE/EMC + EC + $LiPF_6$ is a promising electrolyte to give great safety for lithium secondary batteries.

Hitachi, Limited, Hitachi Research Laboratory, assisted in meeting the publication costs of this article.

References

1. M. Winter, J. O. Besenhard, M. E. Spahr, and P. Novák, *Adv. Mater.*, **10**, 725 (1998).
2. X. Zhang, P. N. Ross, Jr., R. Kostecki, F. Kong, S. Sloop, J. B. Kerr, K. Striebel, E. J. Cairns, and F. McLarnon, *J. Electrochem. Soc.*, **148**, A463 (2001).
3. M. C. Smart, B. V. Batnakumar, S. Surampudi, Y. Wang, X. Zhang, S. G. Greenbaum, A. Hightower, C. C. Ahn, and B. Fultz, *J. Electrochem. Soc.*, **146**, 3963 (1999).
4. M. S. Ding, K. Xu, and T. R. Jow, *J. Electrochem. Soc.*, **147**, 1688 (2000).
5. M. Morita, O. Yamada, M. Ishikawa, and Y. Matsuda, *J. Appl. Electrochem.*, **28**, 209 (1998).
6. C. W. Lee, R. Venkatachalapathy, and J. Prakash, *Electrochem. Solid-State Lett.*, **3**, 63 (1999).
7. D. Peramunage, J. M. Ziegelbauer, and G. L. Holleck, Abstract 144, The Electrochemical Society Meeting Abstracts, Vol. 2000-2, Phoenix, AZ, Oct 22-27, 2000.
8. K. Xu, M. S. Ding, S. Zhang, J. L. Allen, and T. R. Jow, Abstract 118, The 52nd Meeting of the International Society of Electrochemistry, San Francisco, CA (2001).
9. X. Wang, E. Yasukawa, and S. Kasuya, *J. Electrochem. Soc.*, **148**, A1058 (2001).
10. X. Wang, E. Yasukawa, and S. Kasuya, *J. Electrochem. Soc.*, **148**, A1066 (2001).
11. N. Shinoda, J. Ozaki, F. Kita, and A. Kawakami, Abstract 335, The Electrochemical Society and The Electrochemical Society of Japan Meeting Abstract, Vol. 99-2, Honolulu, HI, Oct 17-22, 1999.
12. (a) J. Arai, *J. Appl. Electrochem.*, In press; (b) J. Arai, U.S. Pat. 6,210,835-B1 (2001).
13. J. Arai, H. Katayama, and H. Akahoshi, *J. Electrochem. Soc.*, **149**, A217 (2002).
14. D. Aurbach, Y. Gofer, M. Ben-Zion, and P. Aped, *J. Electroanal. Chem.*, **339**, 451 (1992).
15. D. Aurbach, Y. Ein-Eli, O. Chusid, Y. Carmeli, M. Babai, and H. Yamin, *J. Electrochem. Soc.*, **141**, 603 (1994).
16. S. Shiraishi, K. Kanamura, and Z. Takehara, *J. Electrochem. Soc.*, **146**, 1633 (1999).
17. S. E. Sloop and M. M. Lerner, *J. Electrochem. Soc.*, **143**, 1292 (1996).
18. N. Imanishi, K. Kumai, H. Kokugan, Y. Takeda, and O. Yamamoto, *Solid State Ionics*, **107**, 135 (1998).
19. S. Matsuta, T. Asada, and K. Kitaura, *J. Electrochem. Soc.*, **147**, 1695 (2000).
20. J. S. Gnanaraj, M. D. Levi, E. Levi, G. Salitra, D. Aurbach, J. E. Fischer, and A. Claye, *J. Electrochem. Soc.*, **148**, A525 (2001).
21. D. Aurbach, O. Chusid, I. Weissman, and P. Dan, *Electrochim. Acta*, **41**, 747 (1996).
22. T. Eriksson, A. M. Andersson, G. Bishop, C. Gejke, T. Gustafsson, and J. O. Thomas, *J. Electrochem. Soc.*, **149**, A69 (2002).
23. S. Han, S. K. Koh, and K. H. Yoon, *J. Electrochem. Soc.*, **146**, 4327 (1999).
24. K. Kanamura, T. Umegaki, S. Shiraishi, M. Ohashi, and Z. Takehara, *J. Electrochem. Soc.*, **149**, A185 (2002).
25. L. Péter and J. Arai, *J. Appl. Electrochem.*, **29**, 1053 (1999).
26. L. Péter, J. Arai, and H. Akahoshi, *J. Electroanal. Chem.*, **482**, 125 (2000).